

Pathway Realisability in Chemical Networks

Jakob L. Andersen¹, Sissel Banke^{1*}, Rolf Fagerberg¹, Christoph Flamm^{3,9}, Daniel Merkle^{2,1}, and Peter F. Stadler³⁻⁸

¹Department of Mathematics and Computer Science, University of Southern Denmark, Odense M DK-5230, Denmark

²Algorithmic Cheminformatics Group, Faculty of Technology, Bielefeld University, Bielefeld D-33615, Germany

³Institute for Theoretical Chemistry, University of Vienna, Wien A-1090, Austria

⁴Department of Computer Science, and Interdisciplinary Center for Bioinformatics, University of Leipzig, Leipzig D-04107, Germany

⁵Max Planck Institute for Mathematics in the Sciences, Leipzig D-04103, Germany

⁶Fraunhofer Institute for Cell Therapy and Immunology, Leipzig D-04103, Germany

⁷Center for non-coding RNA in Technology and Health, University of Copenhagen, Frederiksberg C DK-1870, Denmark

⁸Santa Fe Institute, 1399 Hyde Park Rd, Santa Fe NM 87501, USA

⁹Research Network Chemistry Meets Microbiology, University of Vienna, Wien A-1090, Austria

*Corresponding author. E-mail:banke@imada.sdu.dk

Keywords— Chemical reaction network, directed multi-hypergraph, cheminformatics, Petri net, pentose phosphate pathway

Abstract

The exploration of pathways and alternative pathways that have a specific function is of interest in numerous chemical contexts. A framework for specifying and searching for pathways has previously been developed, but a focus on which of the many pathway solutions are realisable, or can be made realisable, is missing. Realisable here means that there actually exists some sequencing of the reactions of the pathway that will execute the pathway. We present a method for analysing the realisability of pathways based on the reachability question in Petri nets. For realisable pathways, our method also provides a certificate encoding an order of the reactions which realises the pathway. We present two extended notions of realisability of pathways, one of which is related to the concept of network catalysts. We exemplify our findings on the pentose phosphate pathway. Furthermore,

we discuss the relevance of our concepts for elucidating the choices often implicitly made when depicting pathways. Lastly, we lay the foundation for the mathematical theory of realisability.

1 Introduction

Large Chemical Reaction Networks (CRNs) are fundamental to numerous scientific, industrial, and societal challenges. Applications include the analysis of metabolic networks and their regulation in health and biotechnology; optimization of chemical synthesis processes; modelling of molecular ion fragmentation in mass spectrometry; investigation of hypotheses concerning the origins of life; and environmental monitoring of pollutants. Subnetworks with specific properties, often referred to as *pathways*—such as synthetic routes to target molecules or metabolic subsystems—are of particular interest. Thus, the ability to define and identify pathways within a CRN is a central objective in chemical modelling, exploration, and design.

CRNs can be modelled as directed hypergraphs [Zeigarnik, 2000, Müller et al., 2022, Andersen et al., 2020, 2019], where vertices represent molecules and directed hyperedges represent reactions. By considering pathways in CRNs as sets of reactions with integer multiplicities, [Andersen et al., 2019] formally defined pathways as integer hyperflows in hypergraphs. The integer hyperflow model for pathways is analogous to flux balance analysis (FBA), another method for pathway discovery. Both approaches enforce mass conservation and typically employ linear constraints to identify pathways. However, they differ in several respects; see [Andersen et al., 2019] for a detailed discussion. Notably, FBA yields flux distributions, whereas integer hyperflows provide pathways as sets of reactions with integer stoichiometric coefficients, facilitating a mechanistic understanding of the pathway. Additionally, [Andersen et al., 2019] introduced the concept of a *chemical transformation motif* in a CRN, offering a flexible framework for querying reaction networks for pathways. A chemical transformation motif specifies a pathway by prescribing the input and output compounds, allowing intermediate products that must be consumed entirely. Computationally, finding and enumerating pathways that fulfil a chemical transformation motif can be addressed via Integer Linear Programming (ILP) [Andersen et al., 2019]. Although ILP is NP-hard in general and even in the restricted context of finding integer hyperflows in CRNs [Andersen et al., 2012], current ILP solvers perform well for many practically relevant networks and pathways [Andersen et al., 2019].

While integer hyperflows specify reactions and their multiplicities, they do not determine the sequence in which these reactions occur to achieve the overall chemical transformation. Indeed, a valid sequencing may not exist. Figure 6 illustrates such a scenario: no ordering of reactions e_1 and e_2 in the

integer hyperflow renders it executable—essentially, molecules C or D must be present prior to their production. We introduce the term *realisable* for integer hyperflows where the corresponding chemical transformation can be executed by some sequence of constituent reactions. To address this, we develop a framework that converts integer hyperflows into corresponding Petri nets, enabling the application of Petri net methodologies to express and determine the realisability of integer hyperflows. Petri nets have been extensively employed to model various aspects of metabolic networks [Baldan et al., 2010].

For realisable integer hyperflows, we introduce the concept of a *realisability certificate*, which specifies an execution order for the reactions along the pathway. Determining an explicit sequence not only enhances mechanistic understanding but is also essential for studies where individual atom identities are important, such as computing atom traces [Andersen et al., 2014]. We also explore methods to extend non-realisable integer hyperflows into realisable ones. One approach involves scaling the integer hyperflow, while another entails borrowing additional molecules that are subsequently returned. This latter method is closely related to the concept of a “network catalyst” (see e.g. [Braakman and Smith, 2013, Morowitz et al., 2008]). An algorithmic approach to deciding realisability through borrowing thus serves as a crucial foundation for future computational treatments of higher-level chemical motifs like autocatalysis and hypercycles [Eigen, 1971, Eigen and Schuster, 1977, Szathmáry, 1988, 2013]. Finally, we apply our methodology to the non-oxidative phase of the pentose phosphate pathway (PPP) to demonstrate its utility and to explore potential catalysts within the network. The PPP is a well-known example that underscores the importance of simplicity in solution finding [Noor et al., 2010, Meléndez-Hevia and Isidoro, 1985].

The primary focus of our paper is the formal definition and exploration of the realisability of pathways. It is noteworthy that conventional representations of pathways in the life sciences literature often reside between the two extremes of integer hyperflows and realisability certificates. We believe that our formalisation of these concepts can raise awareness of the implicit choices made when depicting pathways. This perspective is further elaborated in Section 5.

The remainder of this paper is organised as follows. Section 2 presents the notation and definitions for directed hypergraphs, integer hyperflows, and Petri nets, with terminology following [Andersen et al., 2019]. Section 3 defines the realisability problem, outlines our method for converting integer hyperflows into Petri nets, and introduces realisability certificates. In Section 4, we investigate methods for rendering non-realisable integer hyperflows realisable, either by scaling the hyperflow or by borrowing molecules. Section 5 discusses the implications of integer hyperflows and realisability certificates in pathway depiction. Section 6 examines the mathematical

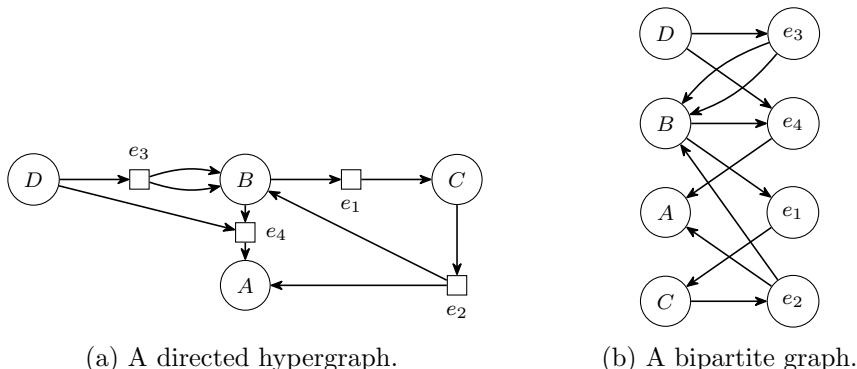


Figure 1: A directed hypergraph in (a) and the corresponding bipartite graph in (b).

properties of pathway realisability.

2 Preliminaries

2.1 Chemical Reaction Networks and Pathways

In this paper we follow [Andersen et al., 2019] and model CRNs as directed hypergraphs. A directed hypergraph $\mathcal{H} = (V, E)$ has a set V of vertices representing the molecules. Reactions are represented as directed hyperedges E , where each edge $e = (e^+, e^-)$ is an ordered pair of multisets of vertices, i.e., $e^+, e^- \subseteq V$.¹ We call e^+ the *tail* of the edge e , and e^- the *head*. In the interest of conciseness we will refer to directed hypergraphs simply as hypergraphs, directed hyperedges simply as edges, and CRNs as networks. For a multiset Q and an element q we use $m_q(Q)$ to denote its multiplicity, i.e., the number of occurrences of q in Q . When denoting multisets we use the notation $\{\{ \dots \}\}$, e.g., $Q = \{\{a, a, b\}\}$ is a multiset with $m_a(Q) = 2$ and $m_b(Q) = 1$. For a vertex $v \in V$ and a set of edges A we use $\delta_A^+(v)$ and $\delta_A^-(v)$ to denote respectively the set of out-edges and in-edges of v contained in A , i.e., the edges in A that have v in their tail and v in their head, respectively. We note that hypergraph modelling is equivalent to the more common modelling via a bipartite species-reactions graph [Fagerberg et al., 2013]. Fig. 1 shows a directed hypergraph in (a) and its equivalent bipartite graph in (b). The hypergraph modelling can be said to provide a slightly stronger distinction between molecules and reactions and it forms the basis of the modelling of hyperflows in [Andersen et al., 2019], on which we build.

To model pathways [Andersen et al., 2019] defines the *extended hypergraph*. Given a hypergraph $\mathcal{H} = (V, E)$ the extended hypergraph is

¹When comparing a multiset M and a set S , we view M as a set. I.e., $M \subseteq S$ holds if every element in M is an element of S .

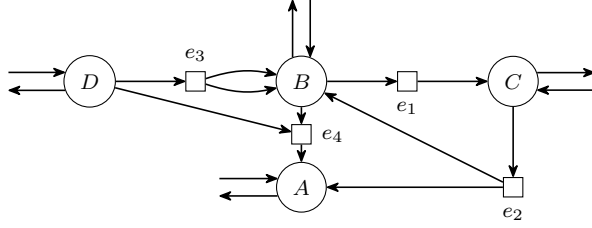


Figure 2: Example of an extended hypergraph. It has vertices $\{A, B, C, D\}$, edges $\{e_1, e_2, e_3, e_4\}$, and a half-edge to and from each vertex. An edge e is represented by a box with arrows to (from) each element in e^- (e^+).

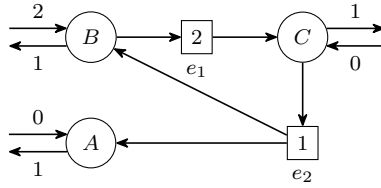


Figure 3: Example flow f on the extended hypergraph from Fig. 2. Vertex D has been omitted as it has no in- or out-flow. Edges leaving or entering D have also been omitted as they have no flow. The flow on an edge is represented by an integer. For example, the half edge into B has flow $f(e_B^-) = 2$, the half edge leaving B has flow $f(e_B^+) = 1$, and edge e_1 has flow $f(e_1) = 2$.

$\overline{\mathcal{H}} = (V, \overline{E})$ with $\overline{E} = E \cup E^- \cup E^+$, where

$$E^- = \{e_v^- = (\emptyset, \{\{v\}\}) \mid v \in V\} \quad E^+ = \{e_v^+ = (\{\{v\}\}, \emptyset) \mid v \in V\} \quad (1)$$

The hypergraph $\overline{\mathcal{H}}$ has additional ‘‘half-edges’’ e_v^- and e_v^+ , for each $v \in V$. These explicitly represent potential input and output channels to and from \mathcal{H} , i.e., what is called exchange reactions in metabolic networks. An example of an extended hypergraph is shown in Fig. 2.

An *integer hyperflow* is an integer-valued function f on the extended network, $f: \overline{E} \rightarrow \mathbb{N}_0$, which satisfies the following *flow conservation constraint* on each vertex $v \in V$:

$$\sum_{e \in \delta_{\overline{E}}^+(v)} m_v(e^+)f(e) - \sum_{e \in \delta_{\overline{E}}^-(v)} m_v(e^-)f(e) = 0 \quad (2)$$

Note in particular that $f(e_v^-)$ is the input flow for vertex v and $f(e_v^+)$ is its output flow. We will for the remainder of the paper refer to integer hyperflows simply as flows. An example of a flow is shown in Fig. 3.

2.2 Petri Nets

Petri nets are an alternative method to analyse CRNs. Each molecular species in the network forms a *place* in the Petri net and each reaction corresponds to a transition [Koch, 2010, Reddy et al., 1993, 1996]. The stoichiometric matrix commonly used in chemistry has an equivalent in Petri net terminology, called the incidence matrix [Koch, 2010]. In Section 3 we will describe a transformation of a flow to a Petri net. The following notation for Petri nets (with the exception of arc weights) follows [Esparza, 1998].

A *net* is a triple (P, T, W) with a set of places P , a set of transitions T , and an arc weight function $W: (P \times T) \cup (T \times P) \rightarrow \mathbb{N}_0$. A *marking* on a net is a function $M: P \rightarrow \mathbb{N}_0$ assigning a number of tokens to each place. With M_\emptyset we denote the empty marking, i.e., $M_\emptyset(p) = 0, \forall p \in P$. A *Petri net* is a pair (N, M_0) of a net N and an initial marking M_0 . For all $x \in P \cup T$, we define the *pre-set* as $\bullet x = \{y \in P \cup T \mid W(y, x) > 0\}$ and the *post-set* as $x^\bullet = \{y \in P \cup T \mid W(x, y) > 0\}$. We say that a transition t is enabled by the marking M if $W(p, t) \leq M(p), \forall p \in P$. When a transition t is enabled it can *fire*, resulting in a marking M' where $M'(p) = M(p) - W(p, t) + W(t, p), \forall p \in P$. Such a firing is denoted by $M \xrightarrow{t} M'$. A *firing sequence* σ is a sequence of firing transitions $\sigma = t_1 t_2 \dots t_n$. Such a firing sequence gives rise to a sequence of markings $M_0 \xrightarrow{t_1} M_1 \xrightarrow{t_2} M_2 \xrightarrow{t_3} \dots \xrightarrow{t_n} M_n$ which is denoted by $M_0 \xrightarrow{\sigma} M_n$. In Fig. 4 we present an example of a firing sequence which in this instance is the sequence $\sigma = t_1 t_2 t_3$.

3 Realisability of Flows

Andersen et al. [2019] described a method (summarized in Section 2.1) to specify pathways in CRNs and then proceeded to use ILP to enumerate pathway solutions fulfilling the specification. In this paper, we focus on assessing the realisability of such a pathway solution and on determining a specific order of reactions that proves its realisability. To this end, we map flows into Petri nets and rephrase the question of realisability as a particular reachability question in the resulting Petri net.

3.1 Flows as Petri Nets

We convert a hypergraph $\mathcal{H} = (V, E)$ to a net $N = (P, T, W)$ by using the vertices V as the places P and the edges E as the transitions T , and by defining the weight function from the incidence information as follows: for each vertex/place $v \in V$ and edge/transition $e = (e^+, e^-) \in E$ let $W(v, e) = m_v(e^+)$ and $W(e, v) = m_v(e^-)$. This conversion also works for extended hypergraphs, where the half-edges result in transitions with either an empty pre-set or post-set. The transitions corresponding to input reactions are thus always enabled.

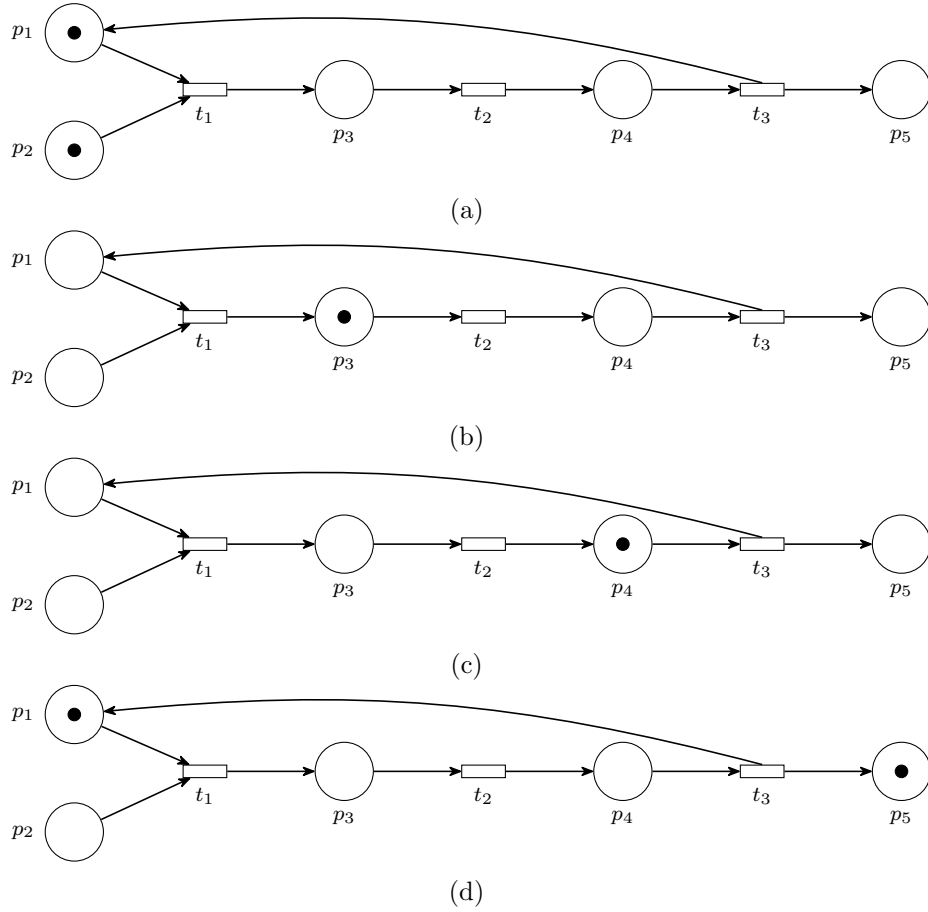


Figure 4: Example firing sequence. Here $P = \{p_1, p_2, p_3, p_4, p_5\}$, $T = \{t_1, t_2, t_3\}$, $W = \{(p_1, t_1) \mapsto 1, (p_2, t_1) \mapsto 1, (t_1, p_3) \mapsto 1, (p_3, t_2) \mapsto 1, (t_2, p_4) \mapsto 1, (p_4, t_3) \mapsto 1, (t_3, p_5) \mapsto 1, (t_3, p_1) \mapsto 1\}$, and the initial marking $M_0 = \{p_1 \mapsto 1, p_2 \mapsto 1, p_3 \mapsto 0, p_4 \mapsto 0, p_5 \mapsto 0\}$ which is depicted in (a). The firing sequence that leads to (d) is $\sigma = t_1 t_2 t_3$, which is illustrated through (a) to (d).

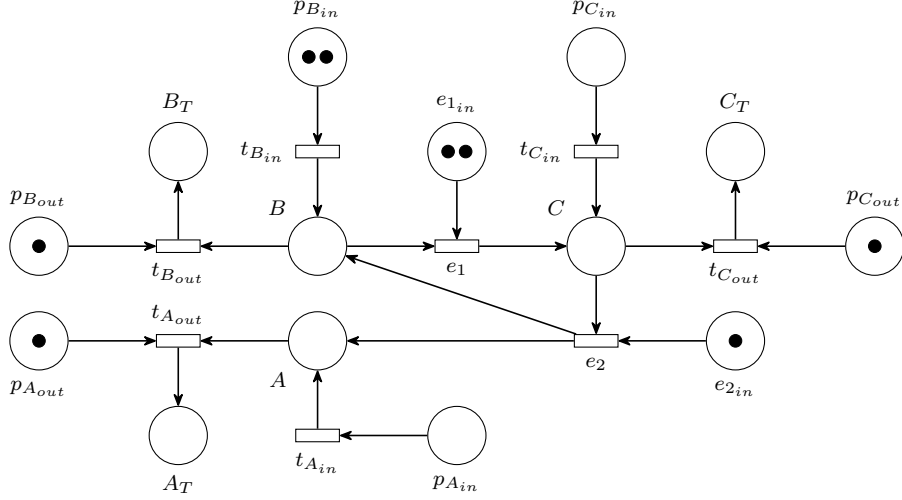


Figure 5: The flow from Fig. 3 converted to a Petri net with its initial marking. Places are circles, transitions are rectangles, and tokens are black dots. Arrows indicate pairs of places and transitions for which the weight function W is non-zero (in this example, all non-zero weights are equal to one). The target marking is $M_T(A_T) = 1$, $M_T(B_T) = 1$, $M_T(C_T) = 1$ and $M_T(p) = 0$ for all $p \in P \setminus \{A_T, B_T, C_T\}$. We have omitted the part of the net that corresponds to the omitted part of Fig. 3.

Given a flow, we would like to constrain the Petri net such that it yields only firing sequences for that particular flow. We therefore further convert the extended hypergraph $\overline{\mathcal{H}}$ into an extended net $(V \cup V_E \cup V_T, \overline{E}, W \cup W_E)$ by adding for each edge $e \in \overline{E}$ an “external place” $v_e \in V_E$ with connectivity $W(v_e, e) = 1$ and for each edge $e^+ \in E^+$ adding a “target place” $v_{e^+} \in V_T$ with connectivity $W(e^+, v_{e^+}) = 1$. In the following, we will denote the extended Petri net again by N . We then proceed by translating the given flow f of $\overline{\mathcal{H}}$ into an initial marking M_0 on the extended net. To this end, we set $M_0(v) = 0$ for $v \in V \cup V_T$ and $M_0(v_e) = f(e)$ for places $v_e \in V_E$. Additionally, we set the target marking denoted by M_T to $M_T(v) = 0$ for $v \in V \cup V_E$ and $M_T(v_{e^+}) = f(e^+)$ for places $v_{e^+} \in V_T$.

Transitions in (N, M_0) therefore can fire at most the number of times specified by the flow. Furthermore, any firing sequence $M_0 \xrightarrow{\sigma} M_T$ ending in the target marking must use each transition exactly the number of times specified by the flow. As an example, the flow in Fig. 3 is converted to the Petri net in Fig. 5.

3.2 Realisability of Flows

We are interested in whether a given pathway, represented by a flow f on an extended hypergraph $\overline{\mathcal{H}} = (V, \overline{E})$, is realisable in the following sense:

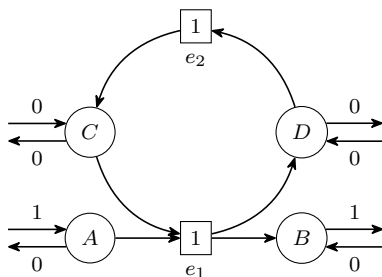


Figure 6: Example of a flow which is not realisable. Observe that the flow is indeed viable as it fulfils the flow conservation constraint. Furthermore, notice that there is no input flow to neither C nor D , and therefore in the corresponding Petri net it will not be possible to fire either of e_1 or e_2 which is necessary for it to be realised. However, if C or D was borrowed the related flow with this borrowing would be realisable.

Given the input molecules specified by the input flow, is there a sequence of reactions that respects the flow, which in the end produces the output molecules specified by the output flow? In the light of the construction of (N, M_0) from $(\overline{\mathcal{H}}, f)$, this question translates into a reachability problem on a Petri net.

Definition 3.1. A flow f on $\overline{\mathcal{H}}$ is realisable if there is a firing sequence $M_0 \xrightarrow{*} M_T$ on the Petri net (N, M_0) constructed from $(\overline{\mathcal{H}}, f)$.

Fig. 6 shows that not all flows f on $\overline{\mathcal{H}}$ are realisable. In this example it is impossible to realise the flow as long as there is no flow entering either C or D . For the flow in Fig. 3, on the other hand, such a firing sequence exists. The firing sequences corresponding to a realisable flow are not unique in general. For instance, the Petri net constructed from the flow presented in Fig. 5 can reach the target marking M_T in essentially two different manners. Modulo the firing of input/output transitions, those two firing subsequences are $e_1e_1e_2$ and $e_1e_2e_1$. For a chemical example of a realisable flow see Fig. 7. This is a flow for the formose reaction.

3.3 Realisability Certificate

In order to introduce realisability certificates that describe the causal order of the reactions needed to make the pathway realisable, we need some established terminology.

Definition 3.2 (Occurrence Net [Goltz and Reisig, 1983]). A net $K = (P_K, T_K, F_K)$ with $F_K \subseteq (P_K \times T_K) \cup (T_K \times P_K)$ is an occurrence net iff

1. $\forall x, y \in P_K \cup T_K x F_K^+ y \Rightarrow \neg(y F_K^+ x)$ (F_K^+ denoting the transitive closure of F_K);

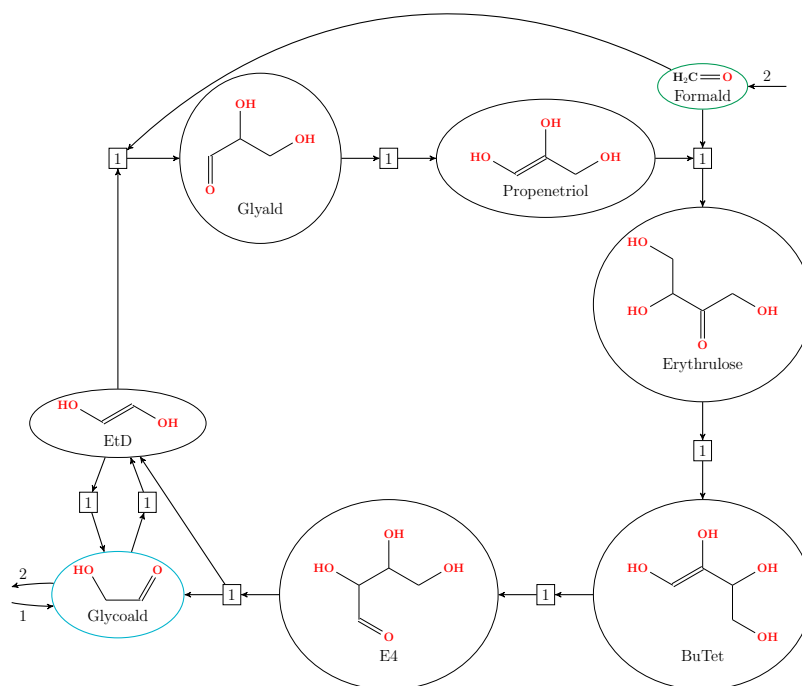


Figure 7: An example of a flow for the formose reaction which is realisable. The input compound Formald is marked with green and Glycoal which is both an input and output compound is marked with turquoise.

$$2. \forall p \in P_K \ | \bullet p| \leq 1 \wedge |p \bullet| \leq 1.$$

“Occurrence net” is also defined in [Genrich and Stankiewicz-Wiechno, 1980, Best and Merceron, 1982], but is used with a different meaning in other sources, see e.g. [Nielsen et al., 1981].

Definition 3.3 (Process [Goltz and Reisig, 1983] (adapted)). Let $N = (P_N, T_N, W_N, M_0)$ be a Petri net and M a reachable marking in N . A *process* is a pair (K, q) of an occurrence net $K = (P_K, T_K, F_K)$ and a mapping $q: K \rightarrow N$ which starts in M and satisfies the following properties

1. $q(P_K) \subseteq P_N$ and $q(T_K) \subseteq T_N$;
2. If $C := \{x \in P_K \mid \bullet x = \emptyset\}$ then $M(p) = |q^{-1}(p) \cap C|$ for all $p \in P_N$;
3. $W_N(p, q(t)) = |q^{-1}(p) \cap \bullet t|$ and $W_N(q(t), p) = |q^{-1}(p) \cap t \bullet|$ for all $t \in T_K$ and $p \in P_N$.

A process is thus an occurrence net that maps back to a Petri net, such that it respects the transitions, places and weight function of the Petri net. Furthermore, the process starts at the marking M in the net.

Definition 3.4. A *realisability certificate* for $(\overline{\mathcal{H}}, f)$ is a process for the Petri net (N, M_0) constructed from $(\overline{\mathcal{H}}, f)$ that leads from the initial marking M_0 to the target marking M_T .

A realisability certificate exists if and only if the target marking M_T is reachable from the initial marking M_0 [Goltz and Reisig, 1983, Theorem 3.6].

A realisability certificate can be constructed from the initial marking using an algorithm exemplified in [Goltz and Reisig, 1983]. Furthermore, the Petri net tool *A Low Level Analyzer* (LoLA)[Schmidt, 2000] is, given a Petri net with its initial marking and a target marking, able to compute a so-called witness path, which is an object isomorphic to a realisability certificate (or tell if the target marking is unreachable and no realisability certificate exists). The computational complexity of reachability in Petri nets is a complex question in the general case [Mayr, 1981, Reutenauer, 1990]. However, in practical cases LoLA performs well—in particular, in our use cases it normally finishes in less than 10 minutes. In this paper, we used LoLA to produce the underlying certificate for our figures. For an example of a realisability certificate see Fig. 8, which is a certificate for the flow in Fig. 3. For a more chemical example of a realisability certificate see Fig. 9, which is for the flow in Fig. 7. To draw realisability certificates more concisely we have omitted $q^{-1}(v)$ for all $v \in V_E \cup V_T$, i.e., the places in the occurrence net that correspond to the external or target places in the Petri net, as well as $q^{-1}(v_e, e)$ for all $v_e \in V_E$ and $q^{-1}(e^+, v_{e^+})$ for all $v_{e^+} \in V_T$, i.e., the arcs leaving the external places or entering the target places in the Petri

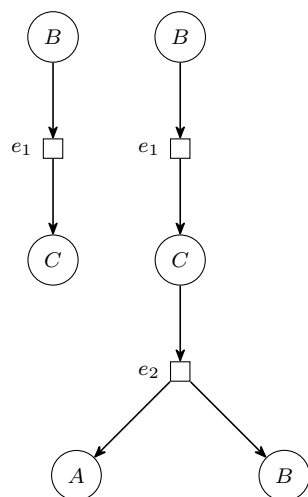


Figure 8: A realizability certificate for the flow in Fig. 3.

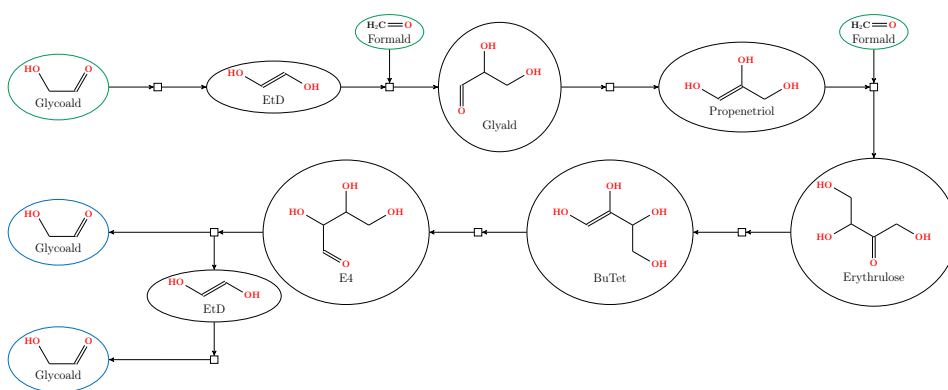


Figure 9: A realizability certificate for the flow in Fig. 7. The input compounds are marked with green and the output compounds are marked with blue.

net. We have also omitted transitions on which the corresponding edges have no flow and places corresponding to vertices with no in- nor out-flow.

A realisability certificate is a directed acyclic graph (DAG) by Def. 3.2 (1), hence it has a topological sorting [Cormen et al., 2009], i.e., a linear ordering of the vertices such that for every edge (u, v) , u comes before v in the ordering. Such a topological sorting of the realisability certificates produces one possible firing sequence of its transitions which realises the flow.

Finally, we note that a realisability certificate is formulated in the Petri net literature such that it gives an individual token interpretation, where individual tokens are distinguishable [van Glabbeek, 2005]. Such a property is an advantage (actually, a necessity) if one is to do atom tracing [Andersen et al., 2014] of stable isotope atoms through the pathway.

4 Extended Realisability

We have demonstrated above that flows may not be realisable. In this section, we study various means by which non-realisable flows may be made realisable.

Definition 4.1 (Scaled-Realisable). A flow f on an extended hypergraph $\overline{\mathcal{H}} = (V, \overline{E})$ is *scaled-realisable*, if there exists an integer $k \geq 1$ such that the resulting flow $k \cdot f$ is realisable.

Asking if a flow f is scaled-realisable corresponds to asking if k copies of f can be realised concurrently. This is of interest as in the real world, a pathway is often not just happening once, but multiple times. Therefore, even if the flow is not realisable, it is meaningful to consider if the scaled flow is. Fig. 10 is an example of such a flow which is not realisable itself, but is scaled-realisable by a factor 2. The flow represents an alternative formose reaction. In order to see that this flow is indeed scaled-realisable, see the realisability certificate of the flow in Fig. 11.

However, not all flows are scaled-realisable. A counter-example is the flow presented in Fig. 6: no integer scaling can alleviate the fact that firing e_1 or e_2 requires C or D to be present at the outset. We note that Thm. 3 from Sec. 6 provides an easily checkable condition which if true implies that a flow is not scaled-realisable.

Definition 4.2 (Borrow-Realisable). Let f be a flow on an extended hypergraph, $\overline{\mathcal{H}} = (V, \overline{E})$ and let b be a function $b: V \rightarrow \mathbb{N}_0$. Set $f'(e_v^-) = b(v) + f(e_v^-)$ and $f'(e_v^+) = b(v) + f(e_v^+)$ for all $v \in V$, and $f'(e) = f(e)$ for all $e \in E$. Then f is *borrow-realisable* if there exists a function b such that f' is realisable.

We denote b as the *borrowing function* and we say that f' is the flow f where $v \in V$ has been borrowed $b(v)$ times. This models that molecules

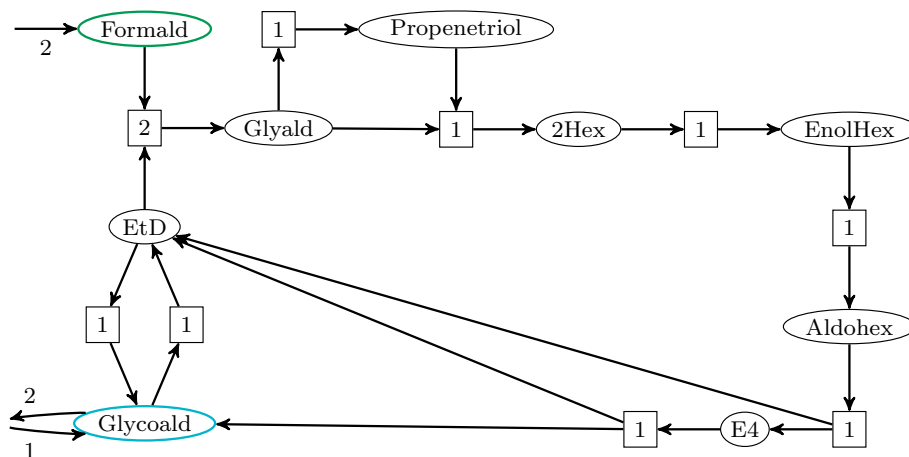


Figure 10: An example of a flow for the formose reaction which is not realisable but is scaled-realisable by a factor 2. The input compound Formald is marked with green and Glycoald which is both an input and output compound is marked with turquoise. The SMILES strings for all molecule identifiers are listed in Appendix, Table 1.

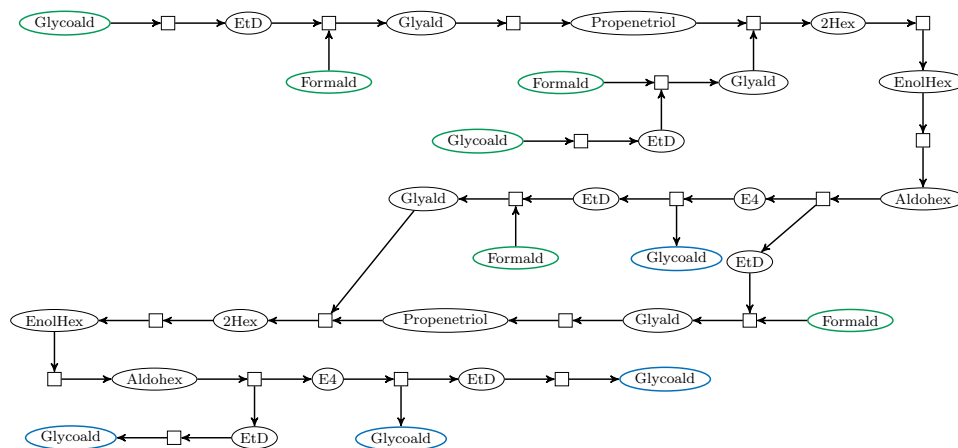


Figure 11: A realisability certificate for the flow in Fig. 10 when scaled by a factor 2, making it scaled-realisable. The input compounds are marked with green and the output compounds are marked with blue. The SMILES strings for all molecule identifiers are listed in Appendix, Table 1.

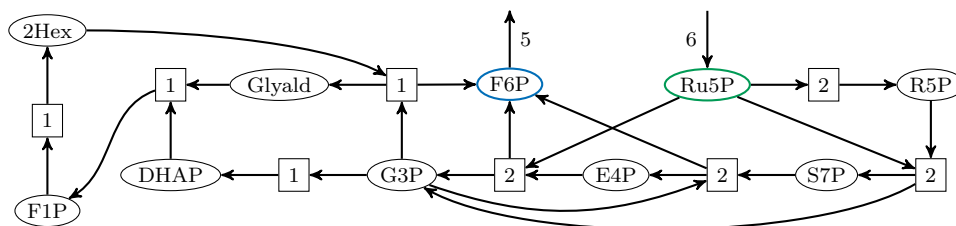


Figure 12: Example of a flow for the pentose phosphate pathway that is not scaled-realizable. The flow is borrow-realizable. The input compound is marked with green and the output compound is marked with blue. The SMILES strings for all molecule identifiers are listed in Appendix, Table 1.

required for reactions in the pathway can be acquired from the environment (and returned afterwards). Formally, this is specified by having an additional input and output flow $b(v)$ for species v . Furthermore, for a borrowing function b we define $|b| = \sum_{v \in V} b(v)$, i.e., the total count of molecules borrowed. The idea of borrowing tokens in the corresponding Petri net setting has been proposed in [Desel, 1998, Proposition 10] together with a theorem which implies that f' is realizable for some b with sufficiently large $|b|$. That is, every flow is in fact borrow-realizable.

The combinatorics underlying the non-oxidative phase of the PPP has been studied in a series of works focusing on simplifying principles that explain the structure of metabolic networks, see e.g. [Noor et al., 2010, Meléndez-Hevia and Isidoro, 1985]. An example of a simple flow from the PPP that is not scaled-realizable is shown in Fig. 12. Here, the production of glyceraldehyde (Glyald) is dependent of the presence of Hex-2-ulose (2Hex), which depends on fructose 1-phosphate (F1P), which in turn depends on Glyald. This cycle of dependencies by Thm. 3 implies that firing is impossible unless one of the molecules in this cycle is present at the outset, which cannot be achieved by scaling. As illustrated in Fig. 13 and proven by the existence of the realisability certificate, the flow is borrow-realizable with just one borrowing, namely of the compound Glyald. Thus Glyald can be seen as a network catalyst for this pathway.

5 Representations of Pathways

We have described two ways of modelling pathways: flows and realisability certificates. The realisability certificate defines a causal order in the pathway and explicitly expresses which individual molecule is used when and for which reaction. A realisability certificate uniquely determines a corresponding flow. Flows, on the other hand, do not specify the order of the reactions or which one of multiple copies of a molecules is used in which reaction. A flow therefore may correspond to multiple different realisability certificates,

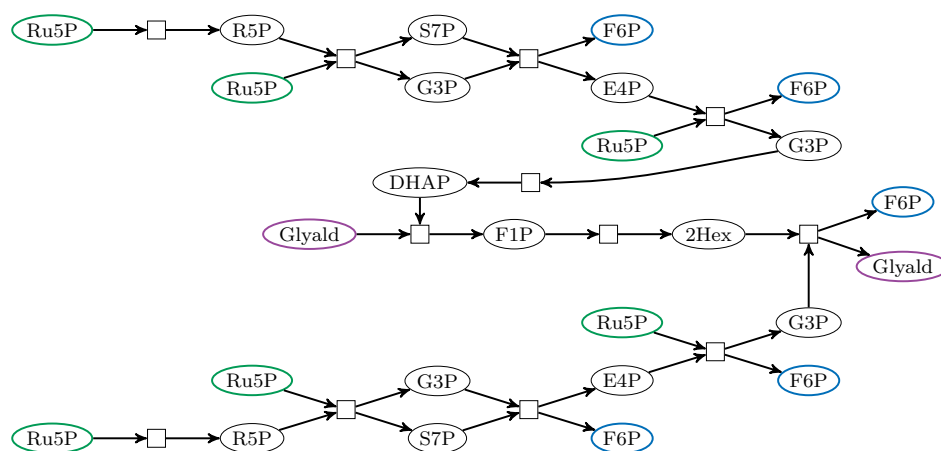


Figure 13: A realisability certificate for the flow in Fig. 12 where the molecule Glyald is borrowed in order to make it borrow-realizable. The input compounds are marked with green, the output compounds are marked with blue and the borrowed compound is marked with purple. The SMILES strings for all molecule identifiers are listed in Appendix, Table 1.

each representing a different mechanism.

We want to point out that commonly used representations of pathways in the life science literature fall in between these two extremes, see Fig. 14 for an example. In this example, the order of reactions is not fully resolved—for instance, is F6P produced before E4P or after? Indeed, some unspecified choice of borrowing is needed to set the pathway in motion. Additionally, the semantics of a molecule identifier appearing in several places is unclear—for instance, are the three appearances of G3P interchangeable in the associated reactions or do they signify different individual instances of the same type of molecule? In the former case, the figure corresponds to a much larger number of different realisability certificates than in the latter case. The answers to these questions have important consequences for investigations where the identity of individual atoms matter, such as atom tracing.

Furthermore, when there is a choice between different pathway suggestions, avoiding borrow-realizable pathways often gives simpler depictions. However, this introduces a bias among the possible pathways, which may be unwanted, as borrow-realizable solutions are usually equally simple in chemical terms. We note that the need for borrowing in pathways is usually not discussed in the literature. Additionally, there has been a lack of computational methods to systematically look for borrow-realizable pathways, even if they could equally likely form part of what happens in nature. For instance, the PPP is usually depicted in a form that give rise to a realisable flow depicted in Fig. 15, with a realisability certificate shown in Fig. 16. It could just as well be described by the equally simple and chemically realistic

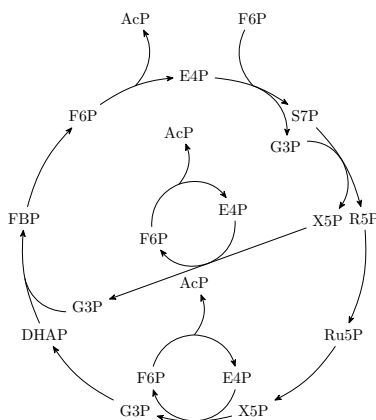


Figure 14: Example of a pathway drawing for the cyclic non-oxidative glycolysis (NOG) pathway. Recreated from [Bogorad et al., 2013, Fig. 2a].

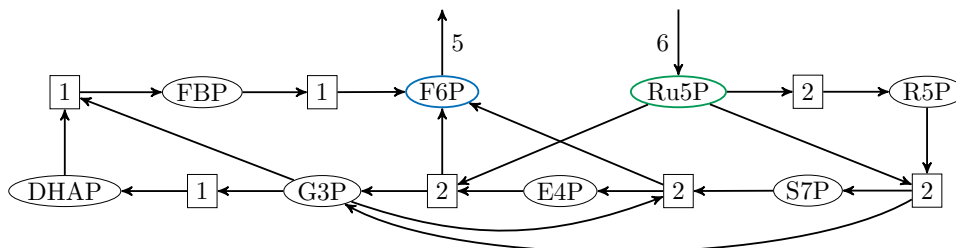


Figure 15: A flow for the pentose phosphate pathway which is realisable. The input compound is marked with green and the output compound is marked with blue. The SMILES strings for all molecule identifiers are listed in Appendix, Table 1.

borrow-realisable pathway depicted in Fig. 12.

We believe that our focus on the realisability of pathways may help raise awareness of the choices one often subconsciously makes when creating pathway illustrations.

6 Mathematical Properties of Realisability

In this section, we take the first steps towards a mathematical theory of the realisability of flows. We begin with a result on realisable flows and prove that if the *König representation* of the *flow-induced subhypergraph* of the extended hypergraph and flow f does not have any cycles, then f is realisable.

Definition 6.1 (Flow-induced Subhypergraph). The flow-induced subhypergraph of an extended hypergraph $\overline{\mathcal{H}} = (V, \overline{E})$ and a flow f is the directed

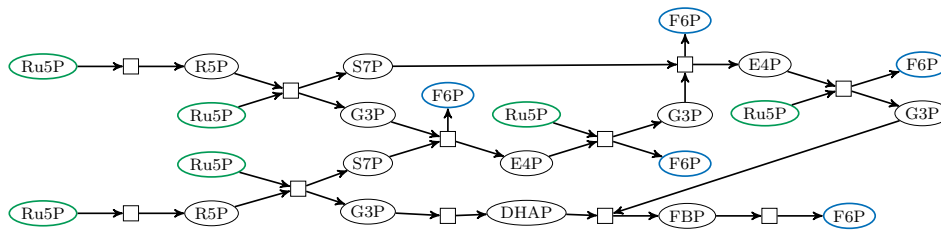


Figure 16: A realisability certificate for the flow in Fig. 15. The input compounds are marked with green and the output compounds are marked with blue. The SMILES strings for all molecule identifiers are listed in Appendix, Table 1.

hypergraph $\overline{\mathcal{H}}[f] = (V', E')$, with

$$\begin{aligned} E' &= \{e \in E \mid f(e) \neq 0\} \\ V' &= \{v \in e^+ \vee v \in e^- \mid e \in E, f(e) \neq 0\} \end{aligned} \quad (3)$$

Definition 6.2 (König Representation [Andersen et al., 2020]). The König representation of a directed hypergraph $\mathcal{H} = (V, E)$ is the directed multi-graph $K(\mathcal{H}) = (V', E')$ where $V' = V \cup E$ and

$$\begin{aligned} E' &= \left\{ \left\{ (v, e) \mid e = (e^+, e^-) \in E, v \in e^+ \right\} \right. \\ &\quad \left. \cup \left\{ (e, v) \mid e = (e^+, e^-) \in E, v \in e^- \right\} \right\} \end{aligned}$$

In short, the König representation of a hypergraph arises simply by considering both the circles and boxes of its visualization (in the style of e.g. Fig. 2) as nodes and the arrows as edges.

Lemma 1. If $K(\overline{\mathcal{H}}[f])$ has no cycles, then f is realisable.

Proof. Since $K(\overline{\mathcal{H}}[f])$ is a DAG, it has a topological sort. Order the nodes of \mathcal{H} on a line according to this. Create nodes for input (output) “half-edges” making them full hyperedges and put these new nodes first (last) in the topological sort. Put the number of tokens specified by the flow on the new input nodes. Create a firing sequence by moving a swepline across the topological sort and fire a hyperedge when the last node in its source (multi)set is passed. Fire it the number of times specified by the multiplicity of the edge. By the definition of a topological sort, the following holds for any node v

- (i) When the swepline reaches v , v has received all its tokens in the flow.
- (ii) Node v only needs to supply tokens after the swepline has reached v .
- (iii) If v is the last node in the sources of a hyperedge, the hyperedge can fire (i.e. there are still enough tokens on every node in its source).

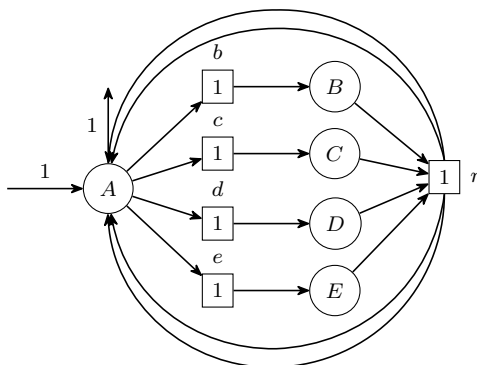


Figure 17: A flow which is not scaled-realizable for an integer $k < 4$ but is for any integer $k \geq 4$.

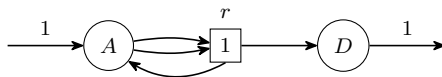


Figure 18: Simple flow that is not scaled-realizable.

Here (i) and (iii) are proven together by induction on the swepline movements and (ii) is true by construction of the firing sequence. \square

There exist flows requiring arbitrary scaling factors:

Theorem 1. For any integer $k > 1$, there exists a flow which is not scaled-realizable for any integer $i < k$ but is scaled-realizable for all integers $i \geq k$.

Proof. One family of such flows is represented by Fig. 17, which fulfils the statement for $k = 4$: This flow is not scaled-realizable for $i < 4$ as all of B, C, D and E need to be present for r to fire in the corresponding Petri net. Therefore, there needs to be at least 4 tokens input to A . To prove that the flow is scaled-realizable for any integer $i \geq 4$, input i tokens to A and output $i - 4$ of them from A , such that 4 tokens still reside on A . Fire the sequence $bcder$. There are now 4 tokens on A again. Repeat the firing of the sequence $bcder$ until it has been fired k times, then output the remaining 4 tokens on A . Clearly, the construction of Fig. 17 generalises to any $k > 1$. If one would like to avoid the unbounded size of the hyperedge r in the family, a binary tree structure can be added on both sides of r (first merging k nodes into one, the expanding this into k nodes connected to A). \square

There also exist flows not scaled-realizable for any factor:

Theorem 2. The flow in Fig. 18 is not scaled-realizable for any integer $k \geq 1$.

Proof. Assume that the flow is scaled-realizable for some factor s . In the firing sequence that realizes the flow, consider the point in time just before the k 'th firing of r . Then at most $s + (k - 1)$ tokens on A have been available. For r to now happen the k 'th time at least $2k$ tokens on A have been available (in order to make the necessary firings of r). Hence $s + (k - 1) \geq 2k \Leftrightarrow s - 1 \geq k$. So s executions of r is not possible. \square

We now give an easily checkable condition which if true implies that a flow is not scaled-realizable for any factor. In short, the condition is that at least one vertex of the flow cannot be reached during a graph traversal from its source set.

In more detail: Consider a directed hypergraph $\mathcal{H} = (V, E)$. The set $R(H, S)$ of vertices reachable from S in \mathcal{H} is defined by (i) $S \subseteq R(H, S)$ and (ii) if $e^+ \subseteq R(H, S)$ for some $e \in E$, then $e^- \subseteq R(H, S)$. It can be computed using the traversal procedure specified in Alg. 1. Setting $w = \max_{e \in E} |e^+|$, Alg. 1 runs in $O(w|E|^2)$ time, since checking the condition of the “while” loop require $O(w|E|)$ time, and in every iteration, F shrinks by one edge.

Algorithm 1: Traversal of a directed hypergraph

Data: $H = (V, E), S$
 $G \leftarrow S$
 $F \leftarrow E$
while $\exists e \in F: e^+ \subseteq G$ **do**
 $G \leftarrow G \cup e^-$
 $F \leftarrow F \setminus \{e\}$
end
return G

Theorem 3. Given a flow f on an extended hypergraph $\overline{\mathcal{H}} = (V, \overline{E})$, let $\overline{\mathcal{H}}[f] = (V', E')$ be the flow induced subhypergraph and let S be the source set such that

$$S = \{v \in V \mid f(e_v^-) \neq 0\} \tag{4}$$

If there exists a vertex $v \in V'$ that is not returned by the traversal procedure on the graph $\overline{\mathcal{H}}[f]$ and source set S , then the flow f is not scaled-realizable.

Proof. The flow-induced subhypergraph $\overline{\mathcal{H}}[f]$ has as edges the internal edges of $\overline{\mathcal{H}}$ on which there is flow, and as vertices the vertices of $\overline{\mathcal{H}}$ that have either in- or out flow, without regard to the half-edges. The source set S contains the vertices of $\overline{\mathcal{H}}$ with input flow according to f . The traversal specified in Alg. 1 corresponds to having an infinite amount of flow into the vertices in S and no restrictions on the number of times an edge can be followed. Therefore, if a vertex is not reachable from S by Alg. 1, it is

also not reachable in the stricter case, where the search is restricted by the flow specification. Note that the omission of the edges on which there is no flow, as well as the vertices for which all internal edges entering or leaving them has no flow, is crucial in order to let Alg. 1 mimic the operations of a scaled flow. Otherwise, there might be ways of visiting the vertices, which would not be possible if only considering the paths represented by the flow specification. Moreover, observe that the omission of vertices which only have in- and outflow does not affect the result of the algorithm as these would be trivially visited. \square

We remark that Thm. 3 only provides a sufficient condition for determining non-scaled-realizable flows and not a necessary condition. This follows from the the flow in Fig. 18: during graph traversal, this flow will have all its vertices visited, but by Thm. 2 it is not scaled-realizable for any factor.

The property of being scaled-realizable is closed under addition of the scaling factors:

Theorem 4. If a flow f is scaled-realizable for an integer k and an integer l , then it is also scaled-realizable for $k + l$.

Proof. Create a realizability certificate for $(k + l) \cdot f$ as the disjoint union of the realizability certificate for $f' = k \cdot f$ and the realizability certificate for $f'' = l \cdot f$. \square

The family of flows from the proof of Thm. 1 has the following interesting property.

Definition 6.3 (Monotone Scaled-Realizable). A flow f is monotone scaled-realizable iff it is scaled-realizable for all integers $j \geq k$, where k is the smallest factor for which it is scaled-realizable.

A natural question now arises whether all scaled-realizable flows are also monotone scaled-realizable. We did a computer-based search for counter-examples, but found none.

In more detail, we generated several pseudo-random directed hypergraphs in which we found a large number of different flows using the software package *MØD* [Andersen et al., 2016, Andersen, 2018] which has a functionality for executing flow queries for hypergraphs via ILP [Andersen et al., 2019]. We tested these flows for realizability and among the flows not directly realizable, we looked at those which were scaled-realizable with a smallest scale factor $k = 2$ or $k = 3$. If the lowest factor was $k = 2$, we tested if the flow was also scaled-realizable for factor $j = 3$. If the lowest factor was $k = 3$, we tested if the flow was also scaled-realizable for factors j where $3 < j \leq 5$. If so, we by Thm. 4 knew that the flow was monotone scaled-realizable. If not, we would have found a counter-example. Among

the 1688 scaled-realizable flows studied, we found them all to be monotone scaled-realizable.

We thus close this section with the following conjecture:

Conjecture 1. All scaled-realizable flows are monotone scaled-realizable.

7 Conclusion

We introduced here a concept of realizability of a pathway given as an flow by converting the flow to a Petri net. The question of realizability can then be rephrased as a question of reachability in the Petri net, leading to notions of realizable, scaled-realizable, and borrow-realizable flows. The method is essential if one is interested in finding alternative realizable pathways to those already known by chemists. Reachability in Petri nets and equivalent formal systems is an active field of research, see e.g. [Alaniz et al., 2022] and the references therein. Many of the relevant reachability problems $M \xrightarrow{*} M'$ are hard for arbitrary markings. It remains a relevant question for future work to see if restrictions imposed by chemistry, in particular conservation of mass, suffice to make the problems easier.

An interesting direction for future research is extending the framework to allow for atom tracing in CRNs. While current Petri net methods allows us to track individual tokens/molecules [van Glabbeek, 2005], full atom tracing requires enumerating *all* possible firing sequences, i.e., *all* witness paths, which existing Petri net tools do not currently provide. On the other hand, atom-atom mapping, i.e., how atoms rearrange during reactions, is already available through an existing graph transformation framework *MØD* [Andersen et al., 2016, Andersen, 2018]. Such a combination of witness path enumeration and atom-atom mapping is crucial for tracking isotopic labels and understanding reaction mechanisms, and would significantly enhance the model’s applicability in systems chemistry, metabolic engineering, and synthetic biology.

Acknowledgments

An early version of this paper was published as part of the ISBRA: International Symposium on Bioinformatics Research and Applications (ISBRA 2023) [Andersen et al., 2023].

Authorship Contribution Statement

Jakob L. Andersen: Conceptualisation, Methodology, Software, Writing - Original Draft, Writing - Review & Editing, Supervision. Sissel Banke:

Methodology, Writing - Original Draft, Writing - Review & Editing, Visualisation. Rolf Fagerberg: Conceptualisation, Methodology, Writing - Review & Editing, Supervision. Christoph Flamm: Conceptualisation. Daniel Merkle: Conceptualisation, Methodology, Writing - Review & Editing, Supervision. Peter F. Stadler: Conceptualisation, Writing - Review & Editing.

Author Disclosure Statement

The authors have no conflict of interest to declare.

Funding Information

This work is supported by the Novo Nordisk Foundation grant NNF19OC0057834 and by the Independent Research Fund Denmark, Natural Sciences, grant DFF-0135-00420B.

References

- Robert M. Alaniz, Bin Fu1 Fu, Timothy Gomez, Elise Grizzell, Andrew Rodriguez, Robert Schweller, and Tim Wylie. Reachability in restricted chemical reaction networks. Technical report, arXiv, 2022.
- Jakob L. Andersen. MedØIDatschgerl (MØD). <http://mod.imada.sdu.dk>, 2018.
- Jakob L. Andersen, Christoph Flamm, Daniel Merkle, and Peter F. Stadler. Maximizing output and recognizing autocatalysis in chemical reaction networks is NP-complete. *Journal of Systems Chemistry*, 3(1), 2012.
- Jakob L. Andersen, Christoph Flamm, Daniel Merkle, and Peter F. Stadler. 50 Shades of rule composition: From chemical reactions to higher levels of abstraction. In François Fages and Carla Piazza, editors, *Formal Methods in Macro-Biology*, volume 8738 of *Lecture Notes in Computer Science*, pages 117–135, Berlin, 2014. Springer International Publishing. ISBN 978-3-319-10397-6.
- Jakob L. Andersen, Christoph Flamm, Daniel Merkle, and Peter F. Stadler. A software package for chemically inspired graph transformation. In Rachid Echahed and Mark Minas, editors, *Graph Transformation: 9th International Conference, ICGT 2016, in Memory of Hartmut Ehrig, Held as Part of STAF 2016, Vienna, Austria, July 5-6, 2016, Proceedings*, pages 73–88. Springer International Publishing, Cham, 2016. ISBN 978-3-319-40530-8. https://doi.org/10.1007/978-3-319-40530-8_5.

- Jakob L. Andersen, Christoph Flamm, Daniel Merkle, and Peter F. Stadler. Chemical transformation motifs — modelling pathways as integer hyperflows. *IEEE/ACM Transactions on Computational Biology and Bioinformatics*, 16(2):510–523, March 2019. ISSN 1545-5963. <https://doi.org/10.1109/TCBB.2017.2781724>.
- Jakob L. Andersen, Christoph Flamm, Daniel Merkle, and Peter F. Stadler. Defining autocatalysis in chemical reaction networks. *Journal of Systems Chemistry*, 8:121–133, 2020. ISSN 2571-7715. URL <http://www.nls-publishers.com/shop/journal/journal+of+systems+chemistry+2020%2c+volume+8>. TR: <https://arxiv.org/abs/2107.03086>.
- Jakob L. Andersen, Sissel Banke, Rolf Fagerberg, Christoph Flamm, Daniel Merkle, and Peter F. Stadler. On the realisability of chemical pathways. In Xuan Guo, Serghei Mangul, Murray Patterson, and Alexander Zelikovsky, editors, *Bioinformatics Research and Applications*, pages 409–419, Singapore, 2023. Springer Nature Singapore. ISBN 978-981-99-7074-2.
- Paolo Baldan, Nicoletta Cocco, Andrea Marin, and Marta Simeoni. Petri nets for modelling metabolic pathways: A survey. *Natural Computing*, 9: 955–989, 12 2010. <https://doi.org/10.1007/s11047-010-9180-6>.
- Eike Best and Agathe Merceron. Discreteness, k-density and d-continuity of occurrence nets. In Armin B. Cremers and Hans-Peter Kriegel, editors, *Theoretical Computer Science*, pages 73–83, Berlin, Heidelberg, 1982. Springer Berlin Heidelberg. ISBN 978-3-540-39421-1.
- Igor W. Bogorad, Tzu-Shyang Lin, and James C. Liao. Synthetic non-oxidative glycolysis enables complete carbon conservation. *Nature (London)*, 502(7473):693–697, 2013.
- Rogier Braakman and Eric Smith. The compositional and evolutionary logic of metabolism. *Physical biology*, 10(1), 2013.
- Thomas H. Cormen, Charles E. Leiserson, Ronald L. Rivest, and Clifford Stein. *Introduction to algorithms*. The MIT Press, Cambridge, MA, 3. edition, 2009.
- Jörg Desel. Basic linear algebraic techniques for place/transition nets. In *Lectures on Petri Nets I: Basic Models*, pages 257–308. Springer, 1998.
- Manfred Eigen. Selforganization of matter and the evolution of biological macromolecules. *Naturwissenschaften*, 58(10):465–523, 1971.
- Manfred Eigen and Peter Schuster. The hypercycle: A principle of natural self-organization. *Die Naturwissenschaften*, 1977.

- Javier Esparza. Decidability and complexity of petri net problems—an introduction. *Lectures on Petri nets I: Basic models*, pages 374–428, 1998.
- Rolf Fagerberg, Christoph Flamm, Daniel Merkle, Philipp Peters, and Peter F. Stadler. On the complexity of reconstructing chemical reaction networks. *Mathematics in computer science*, 7(3):275–292, 2013.
- H. J. Genrich and E. Stankiewicz-Wiechno. A dictionary of some basic notions of net theory. In Wilfried Brauer, editor, *Net Theory and Applications*, pages 519–531, Berlin, Heidelberg, 1980. Springer Berlin Heidelberg. ISBN 978-3-540-39322-1.
- U. Goltz and W. Reisig. The non-sequential behaviour of petri nets. *Information and Control*, 57(2):125–147, 1983. ISSN 0019-9958. [https://doi.org/10.1016/S0019-9958\(83\)80040-0](https://doi.org/10.1016/S0019-9958(83)80040-0).
- Ina Koch. Petri nets – a mathematical formalism to analyze chemical reaction networks. *Molecular Informatics*, 29(12):838–843, 2010. ISSN 1868-1751. <https://doi.org/10.1002/minf.201000086>.
- Ernst Mayr. Persistence of vector replacement systems is decidable. *Acta informatica*, 15(3):309–318, 1981.
- Enrique Meléndez-Hevia and Angel Isidoro. The game of the pentose phosphate cycle. *Journal of Theoretical Biology*, 117(2):251–263, 1985. ISSN 0022-5193. [https://doi.org/10.1016/S0022-5193\(85\)80220-4](https://doi.org/10.1016/S0022-5193(85)80220-4).
- Harold J. Morowitz, Shelley D. Copley, and Eric Smith. *Core Metabolism as a Self-Organized System*, chapter 20. Protocells. The MIT Press, 2008. ISBN 9780262182683;0262182688;.
- Stefan Müller, Christoph Flamm, and Peter F. Stadler. What makes a reaction network “chemical”? *Journal of cheminformatics*, 14(1):63–63, 2022.
- Mogens Nielsen, Gordon Plotkin, and Glynn Winskel. Petri nets, event structures and domains, part i. *Theoretical Computer Science*, 13(1):85–108, 1981. ISSN 0304-3975. [https://doi.org/10.1016/0304-3975\(81\)90112-2](https://doi.org/10.1016/0304-3975(81)90112-2). Special Issue Semantics of Concurrent Computation.
- Elad Noor, Eran Eden, Ron Milo, and Uri Alon. Central Carbon Metabolism as a Minimal Biochemical Walk between Precursors for Biomass and Energy. *Molecular Cell*, 39(5):809–820, 2010. ISSN 10972765. <https://doi.org/10.1016/j.molcel.2010.08.031>.
- Venkatramana N. Reddy, Michael L. Mavrovouniotis, and Michael N. Liebman. Petri net representations in metabolic pathways. *Proceedings. International Conference on Intelligent Systems for Molecular Biology*, pages 328–36, 1993.

- Venkatramana N. Reddy, Michael N. Liebman, and Michael L. Mavrovouniotis. Qualitative analysis of biochemical reaction systems. *Computers in biology and medicine*, 26(1):9–24, 1996.
- Christophe Reutenauer. *The mathematics of Petri nets*. Prentice-Hall, Inc., USA, 1990. ISBN 0135618878.
- Karsten Schmidt. Lola a low level analyser. In Mogens Nielsen and Dan Simpson, editors, *Application and Theory of Petri Nets 2000*, volume 1825 of *Lecture Notes in Computer Science*, pages 465–474. Springer Berlin Heidelberg, 2000. ISBN 978-3-540-67693-5. https://doi.org/10.1007/3-540-44988-4_27.
- Eörs Szathmáry. A hypercyclic illusion. *Journal of theoretical biology*, 134(4):561–563, 1988.
- Eörs Szathmáry. On the propagation of a conceptual error concerning hypercycles and cooperation. *J. Syst. Chem.*, 4:1, 2013.
- Robert Jan van Glabbeek. The individual and collective token interpretations of petri nets. In Martín Abadi and Luca de Alfaro, editors, *CONCUR 2005 – Concurrency Theory*, pages 323–337, Berlin, Heidelberg, 2005. Springer Berlin Heidelberg. ISBN 978-3-540-31934-4.
- Andrew V. Zeigarnik. On hypercycles and hypercircuits in hypergraphs. *Discrete Math. Chemistry*, 51:377–383, 2000. <https://doi.org/10.1090/dimacs/051/28>.

Appendix

Molecular Structures

We have omitted the structure of molecules for brevity in some examples in the paper. This is a large simplification in comparison to the level of detail handled by our complete framework, which includes a generative approach to creating chemical reaction networks [Andersen et al., 2016]. Each vertex in the directed hypergraphs is an undirected labelled graph representing a molecular structure. Each edge in the directed hyperedge correspond to a Double Pushout (DPO) transformation of such a graph [Andersen et al., 2016]. In Table 1 we present the correspondence between the ID and structure of the compounds used throughout the paper. In Fig. 19 we show an example of a DPO diagram that represents a reaction. Since the spans in the DPO representation in particular define a bijection of the vertices (atoms) in tail and head of an hyperedge, it determines the atom-maps of a reaction.

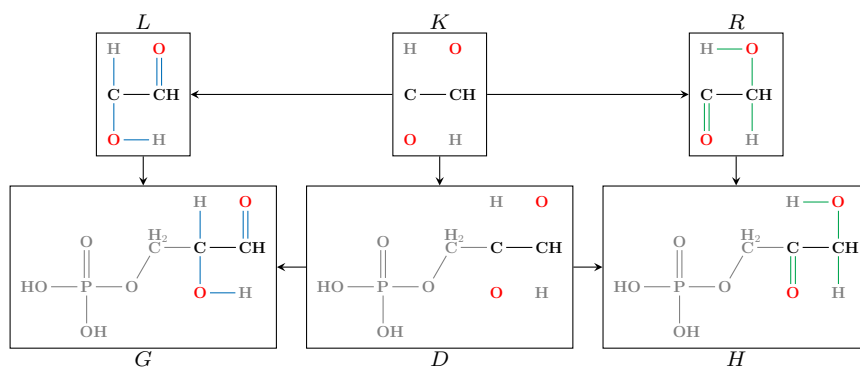


Figure 19: Double Pushout diagram for the edge ($\{\{G3P\}\}$, $\{\{DHAP\}\}$) from Fig. 12. Atoms in corresponding locations are mapped onto each in both the rule (top) and its application to complete molecules (bottom).

Table 1: SMILES strings of the molecules used throughout the paper.

ID	Name	SMILES
2Hex	Hex-2-ulose	<chem>C(CO)(C(C(CO)O)O)O)=O</chem>
Aldohex	Aldohexose	<chem>C(C(C(C(CO)O)O)O)O)=O</chem>
BuTet	1-Butene-1,2,3,4-tetrol	<chem>C(O)=C(C(CO)O)O</chem>
DHAP	Dihydroxyacetone phosphate	<chem>OP(O)(=O)OCC(=O)CO</chem>
E4	Threose	<chem>C(C(C(CO)O)O)=O</chem>
E4P	Erythrose 4-phosphate	<chem>OP(O)(=O)OCC(O)C(O)C=O</chem>
EnolHex	Enol-hexose	<chem>C(O)=C(C(C(CO)O)O)O</chem>
Erythrulose	Erythrulose	<chem>C(CO)(C(CO)O)=O</chem>
EtD	1,2-Ethenediol	<chem>C(O)=CO</chem>
F1P	Fructose 1-Phosphate	<chem>C(COP(O)(O)=O)(C(C(CO)O)O)O)=O</chem>
F6P	Fructose 6-Phosphate	<chem>OCC(=O)C(O)C(O)C(O)COP(=O)(O)O</chem>
FBP	Fructose 1,6-bisphosphate	<chem>OC(COP(O)(O)=O)C(O)C(O)C(COP(O)(O)=O)=O</chem>
Formald	Formaldehyde	<chem>C=O</chem>
G3P	Glyceraldehyde 3-phosphate	<chem>C(C(C=O)O)OP(=O)(O)O</chem>
Glyald	Glyceraldehyde	<chem>C(C(CO)O)=O</chem>
Glycoald	Glycolaldehyde	<chem>OCC=O</chem>
Propenetriol	Prop-1-ene-1,2,3-triol	<chem>C(O)=C(CO)O</chem>
R5P	Ribose 5-phosphate	<chem>OP(O)(=O)OCC(O)C(O)C(O)C=O</chem>
Ru5P	Ribulose-5-Phosphate / Xylulose 5-Phosphate	<chem>OCC(=O)C(O)C(O)COP(=O)(O)O</chem>
S7P	Sedoheptulose 7-phosphate	<chem>O=P(O)(OCC(O)C(O)C(O)C(O)C(=O)CO)O</chem>

Scaled-Realisable Formose Pathway with Molecular Structures

Here we illustrate the scaled-realisable formose pathway from Fig. 10 with molecular structures in Fig. 20 as well as the realisability certificate for said flow from Fig. 11 with the structure of the molecules in Fig. 21.

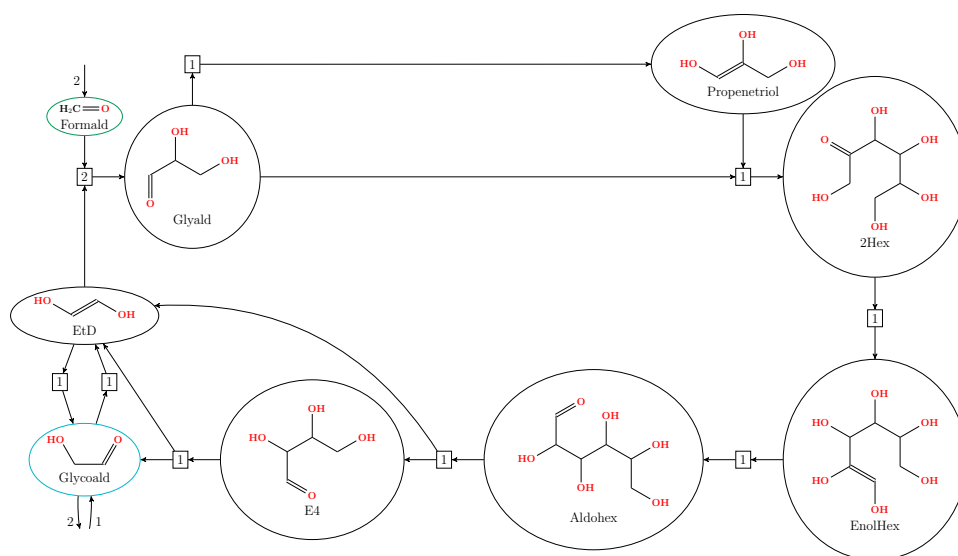


Figure 20: The flow for the formose reaction from Fig. 10 but with molecular structures. It is not realisable but is scaled-realisable by a factor 2. The input compound Formald is marked with green and Glycoald which is both an input and output compound is marked with turquoise.

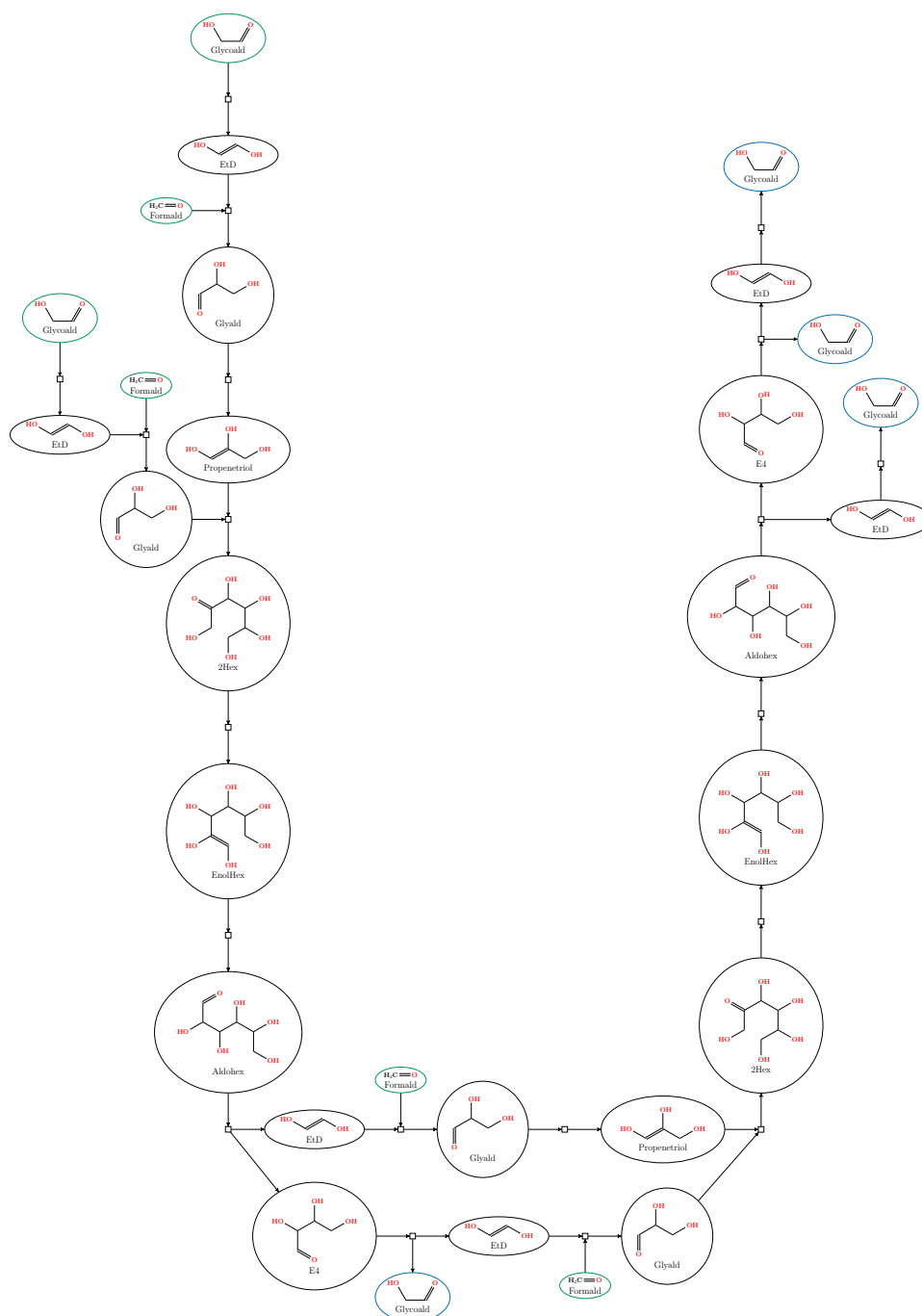


Figure 21: The realisability certificate from Fig. 11 but with the structure of the molecules. The input compounds are marked with green and the output compounds are marked with blue.

Borrow-Realisable Pentose Phosphate Pathway with Molecular Structures

In Fig. 22 we show the borrow-realisable flow for the PPP from Fig. 12 with molecular structures. In Fig. 23 we present a certificate for said flow, also with the structure of the molecules. It is the same certificate as the one from Fig. 13.

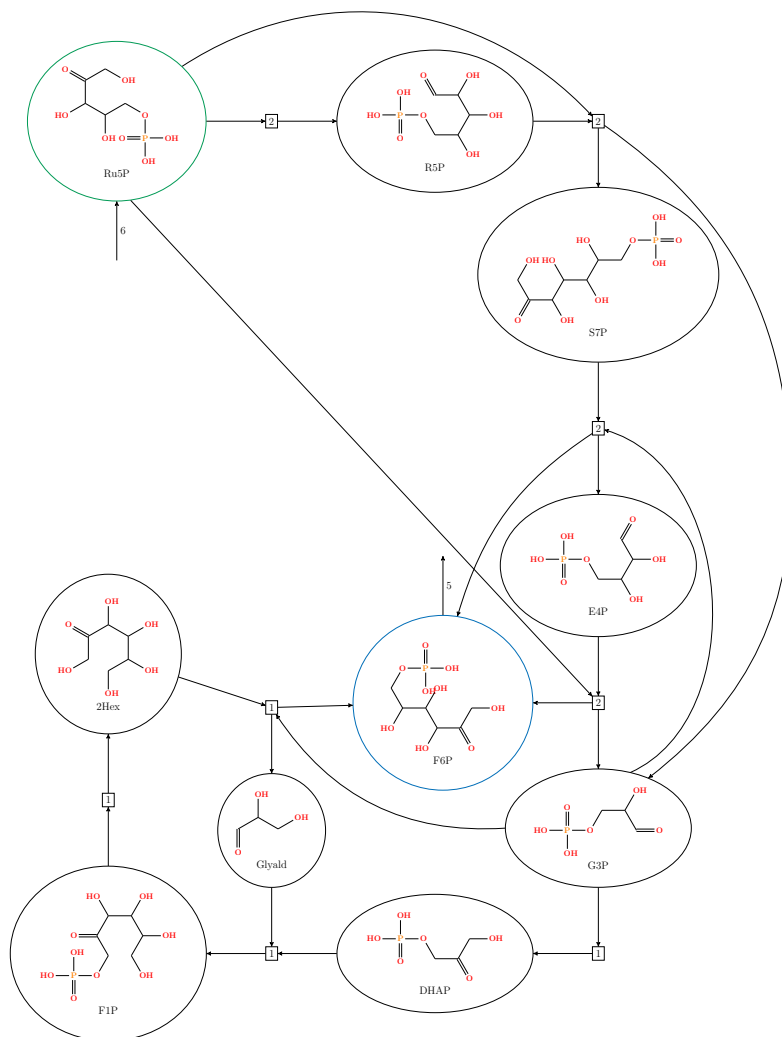


Figure 22: The flow for the PPP from Fig. 12 but with the structure of the molecules. It is not realisable as is but is borrow-realisable. The input compound is marked with green and the output compound is marked with blue.

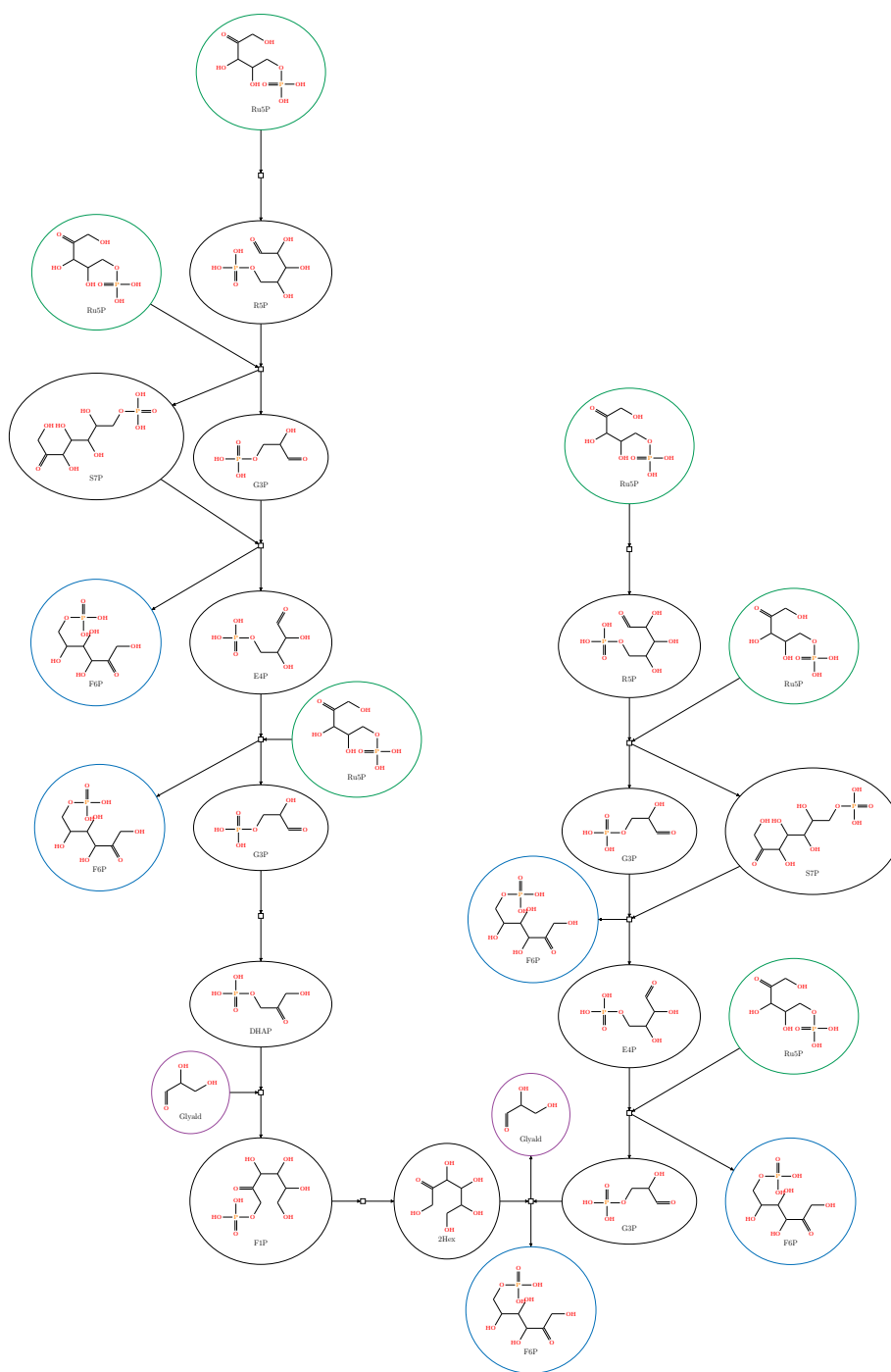


Figure 23: A realisability certificate for the flow in Fig. 22 where the compound Glyald is borrowed. It corresponds to the realisability certificate in Fig. 13 but here the molecular structures are visible. The input compounds are marked with green, the output compounds are marked with blue and the borrowed compound is marked with purple.

Realisable Pentose Phosphate Pathway with Molecular structures

Here we present the flow that depicts a realisable pentose phosphate pathway (PPP) from Fig. 15, but with molecular structures, in Fig. 24 as well as a realisability certificate for it, also with molecular structures, which proves its realisability in Fig. 25.

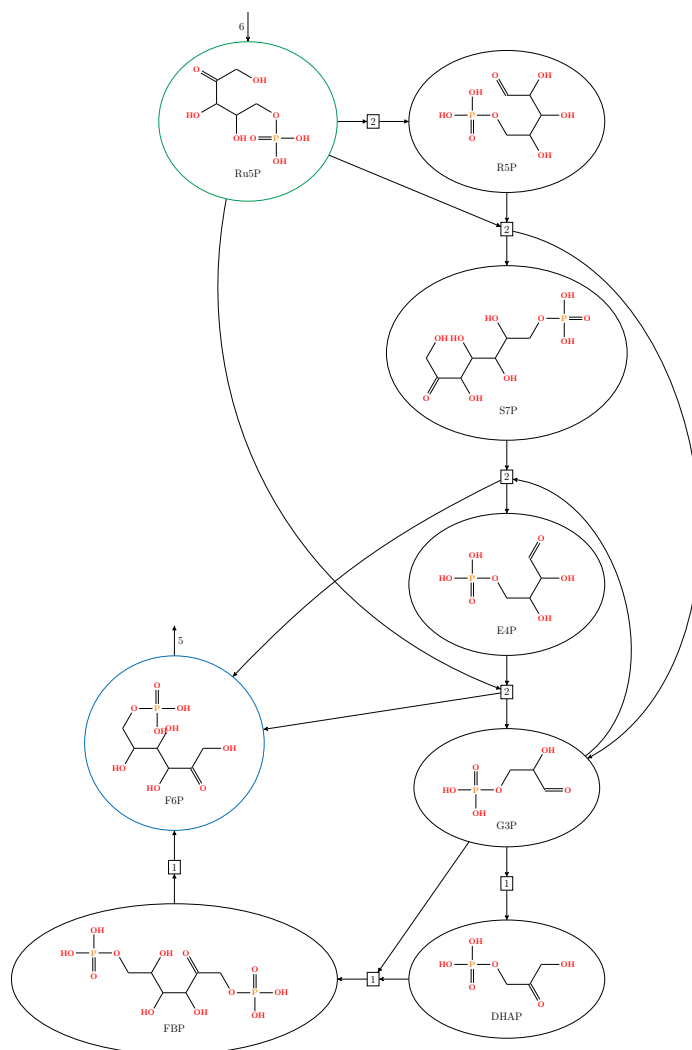


Figure 24: An example of a flow for the pentose phosphate pathway which is realisable. The input compound is marked with green and the output compound is marked with blue.

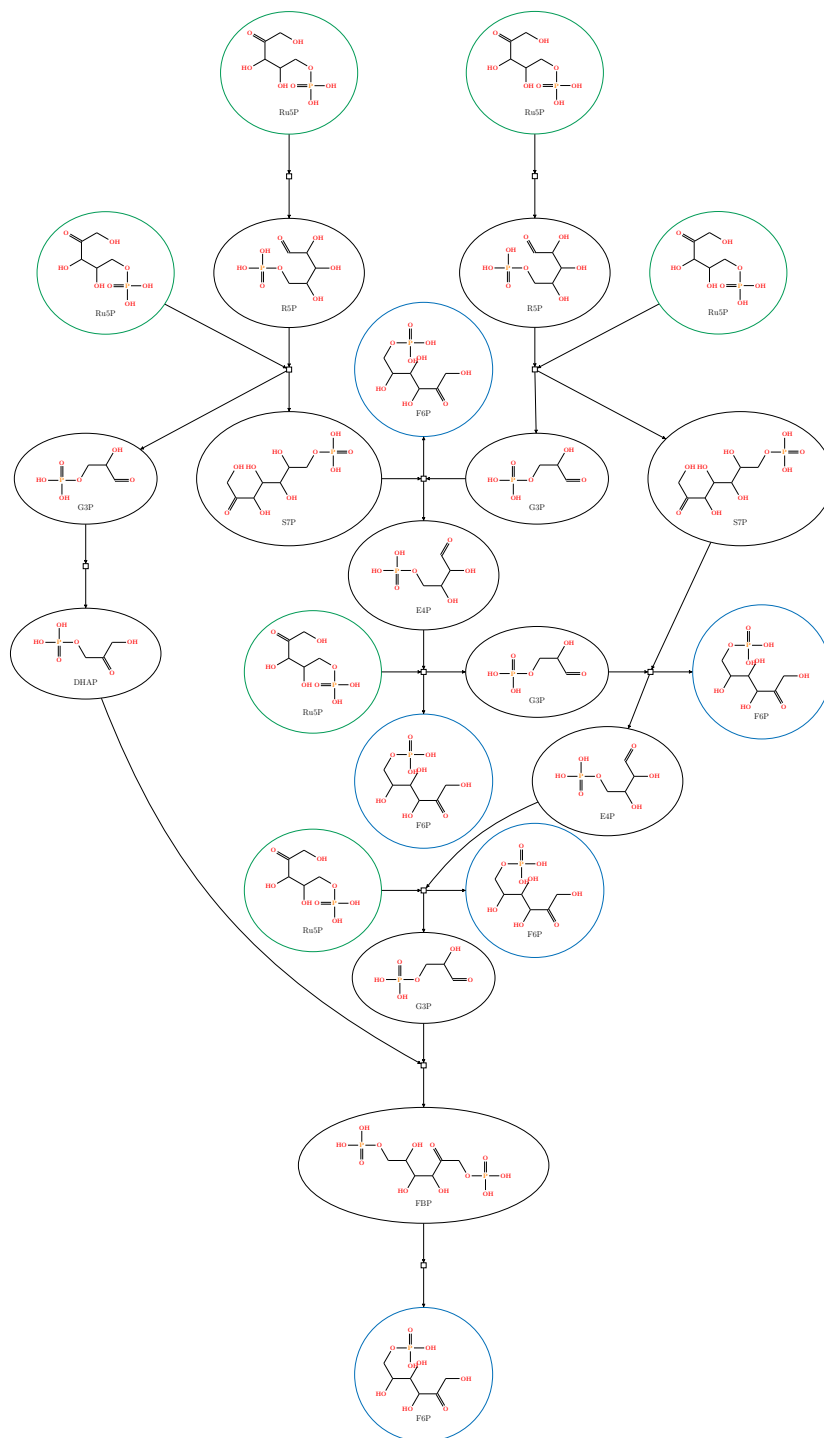


Figure 25: A realisability certificate for the realisable pentose phosphate pathway from Fig. 24. The input compounds are marked with green and the output compounds are marked with blue.